

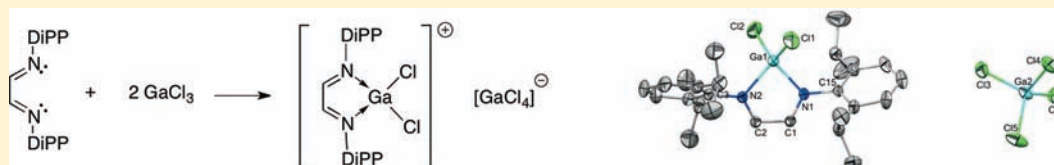
Addition of Aluminum and Gallium Species to Aromatic and Alkyl-Substituted 1,4-Diaza-1,3-butadiene Ligands

Ana M. Felix,[†] Diane A. Dickie,[†] Ian S. Horne,[†] Giang Page,[†] and Richard A. Kemp^{*,†,§}

[†]Department of Chemistry and Chemical Biology, University of New Mexico, Albuquerque, New Mexico 87131-2609, United States

[§]Advanced Materials Laboratory, Sandia National Laboratories, Albuquerque, New Mexico 87106, United States

Supporting Information



ABSTRACT: In this report, we investigate the interactions of $\text{Me}_x\text{MCl}_{3-x}$ ($x = 0-3$, $\text{M} = \text{Al}, \text{Ga}$) with various aromatic and alkyl-substituted 1,4-diaza-1,3-butadiene ^RDAB ligands (or α -diimine ligands) to give a variety of structures in solution and in the solid state. In combination with other previously reported structures, certain general trends of reactivity of these species can be deduced, although there are still some unexplained modes of reactivity. The methylated Al species react with aromatic-substituted ^RDAB ligands to provide final products that result from C=N insertion into the Al-CH₃ group followed by rearrangement reactions. The addition of methyl groups onto the backbone of the ^RDAB ligand is insufficient to stop the insertion and rearrangement processes from occurring. In the case of MeAlCl_2 with the bulky DiPP^RDAB ligand, the reaction could be followed spectroscopically from the monoadduct through the inserted/rearranged final product. Methylated Ga species, however, are much less predictable in their behavior with aromatic-substituted ^RDAB ligands. Depending on the exact species and ratios used, coordinated adducts can be formed and identified, or inserted/rearranged products similar to the aluminum reactions can be obtained. Quite interestingly, cation/anion pairs can also be formed in which GaCl_3 or MeGaCl_2 act as a chloride acceptors. This behavior was unique and substantially different from the analogous Al reactions which formed either a dicoordinated adduct or an inserted/rearranged complex. When the stronger-donating alkyl-substituted ^RDAB ligands were used with Me_2GaCl , only cation/anion pairs were obtained. Surprisingly, when the same reactions were performed using Me_2AlCl as a reagent, irreproducible results were obtained.

INTRODUCTION

Much of the preparative effort put forth by inorganic coordination chemists lies in the conception and syntheses of new ligands designed to affect the metal center in a rational manner. The chemist's desire to specifically control targeted properties of the metal of interest has led to an amazingly broad array of ligand architectures, with significant structural variations in electronic and steric features now commonplace. One such family of donors that has seen widespread use is the family of 1,4-diaza-1,3-butadiene or ^RDAB ligands (also commonly referred to as α -diimines). As one might expect, the vast majority of structural and mechanistic studies using this ligand family involve transition metals or lanthanide elements, primarily for applications in catalysis or luminescence.¹ Several reasons for the significant interest in the ^RDAB ligands have been put forth in a review by van Koten et al.,² and among the features of these ligands that lend synthetic versatility are (a) the inherent flexibility of the ligand backbone, (b) the ability of the ^RDAB framework to act as either a σ -donor or a π -acceptor ligand, and (c) the ability to alter the nature of the ^RDAB ligand by varying the pendant R groups. As mentioned, ^RDAB ligands have been more recently utilized in a variety of catalytic studies, for example, in olefin polymerization catalysis as well as in the

production of CO/olefin copolymers.^{1d-i,3} However, despite the high level of application within transition-metal chemistry, the investigation of the coordination of ^RDAB ligands toward main-group (s and p block) metals has significantly lagged that of the d and f block elements.

Our interest in the ^RDAB family of ligands was initiated over 15 years ago by the desire to prepare olefin polymerization catalysts that contained main-group elements as the active components rather than transition metals. Albeit unsuccessful in achieving the goal of preparing high-activity polymerization catalysts with main-group metals, that preliminary study was the genesis of our more recent investigations of the interactions of various group 13 metal complexes with ligands containing the ^RDAB backbone. We recently reported a unique, multi-chromic ligand/metal complex prepared from Me_2GaCl and DiPP^RDAB (DiPP = 2,6-diisopropylphenyl ligand (this compound will be briefly mentioned later on in this manuscript as compound 12)).⁴ Quite unusually, this compound could provide crystallographically identical materials that were either bright yellow or green in color, or surprisingly, mixed yellow and

Received: November 30, 2011

Published: March 28, 2012

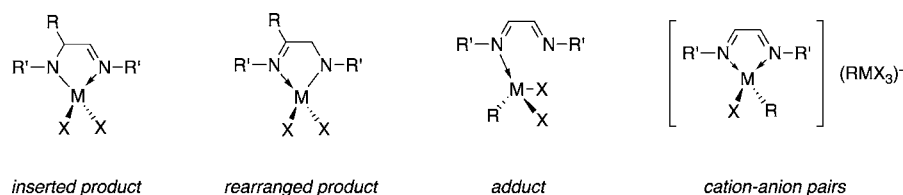


Figure 1. Possible structures arising from interactions of R^DAB ligands with, e.g., group 13 $R-MX_2$ species.

green *within a single crystal*. The presence of a very small amount of a highly colored blue byproduct in the yellow crystal was identified as the likely source for the green color. However, during our prior catalytic investigations, we became intrigued not only by the unusual coloration of the crystals but also by the unusual alkyl transfer and rearrangement reactions that were observed upon the addition of various methylated group 13 species to R^DAB ligands. We note that the transfer and rearrangement behavior was not unprecedented, as this reactivity had first been described by van Koten et al. using Me_3Al and R^DAB ligands in 1979.⁵ However, there has been only a limited number of follow-up reports describing this unusual reactivity using main group metals, certainly when compared to the considerable number of transition-metal- R^DAB studies that have been reported. These more recent main-group studies will be noted and described in context when appropriate within the Results and Discussion section (*vide infra*), but in some cases these reports consist only of single crystal X-ray structures.

It was of interest to us to investigate more fully the range of group 13 compounds that might undergo this transfer reaction, as well as to expand the substituent types that can be used as R^DAB modifiers. We were also interested in observing whether the unusual multicolored nature of the crystals described above was unique and singular, or whether related members of the R^DAB -group 13 family of compounds might also exhibit this unusual feature. This contribution reports the synthesis and analytical characterization, including X-ray structural studies, for the products of Al- and Ga-based complexes with both aryl- and alkyl-substituted R^DAB ligands. Reaction pathways resulting in either methyl group transfer-rearrangement reactions or simple Lewis acid–base adduct formation were both observed for aromatic-substituted R^DAB ligands, as well as unusual examples of cation/anion complexes (Figure 1). However, with alkyl-substituted R^DAB ligands using Me_2GaCl , we observed only the formation of cation/anion pairs. While highly interesting main-group complexes of cyclic ligands related to R^DAB ligands such as bis(imino)acenaphthenes (BIAN) have been recently prepared and investigated,⁶ we have chosen to limit our work to these more simply substituted R^DAB ligands.

EXPERIMENTAL SECTION

General. Standard glovebox and vacuum line techniques were used, as all reagents and products other than the starting diimines are highly air- and/or moisture-sensitive.⁷ The protio-backbone versions of the substituted R^DAB ligands containing $R = 2,4,6$ -trimethylphenyl (Me^sDAB),⁸ 2,6-dimethylphenyl ($2,6Me^2PhDAB$),⁹ 2,6-di-*i*-propylphenyl (Di^iPPDAB),⁹ *t*-butyl (t^BuDAB),¹⁰ or cyclohexyl ($CHexDAB$)¹⁰ were prepared as reported previously in the literature, as was the DiPP-containing dimethylated backbone ligand [$Di^iPPDAB(Me_2)$].⁹ $MeAlCl_2$, $MeGaCl_2$, and Me_2GaCl were prepared according to published procedures.¹¹ Anhydrous solvents were purchased from Aldrich and were used without further purification. All other reagents were purchased from commercial sources including Aldrich, Strem, and Gelest and used without further purification. Molecular sieves were

added to the deuterated solvents to provide additional drying. Solution NMR spectral data were collected either on a Bruker AC 250 MHz spectrometer with a Tecmag MacSpect upgrade or a Bruker Avance III 300 MHz spectrometer at the University of New Mexico NMR Laboratory. Chemical shifts are reported in parts per million (ppm) downfield from $SiMe_4$ and were calibrated to the residual protic signal of the deuterated solvent. Melting points were measured under argon using a Uni-Melt capillary melting point apparatus and are reported uncorrected. Elemental analyses were obtained from Columbia Analytical Services located in Tucson, Arizona. *We do note that many of the isolated compounds reported here will darken and discolor upon prolonged storage if they contain impurities.*

Synthesis of (1). Di^iPPDAB (0.50 g, 1.32 mmol) was added slowly to a colorless solution of $MeAlCl_2$ (0.15 g, 1.32 mmol) in toluene (5 mL). The solution turned bright red immediately. The reaction was stirred overnight at rt, during which time a white precipitate formed. The product was isolated by filtration, and the supernatant was cooled to $-25\text{ }^\circ\text{C}$ to obtain additional product as X-ray-quality single crystals. Yield: 52% (0.34 g), mp $> 200\text{ }^\circ\text{C}$. 1H NMR (300 MHz, δ , in C_6D_6): 7.19–7.22 (m, 3H, (*i*-Pr) $_2C_6H_3$), 6.97–7.08 (m, 3H, (*i*-Pr) $_2C_6H_3$), 4.02 (br s, 2H, $N=C(Me)-CH_2-N$), 3.78 (sept, 2H, $J = 6.9$ Hz, $CHMe_2$), 3.07 (sept, 2H, $J = 6.6$ Hz, $CHMe_2$), 1.44 (d, 6H, $J = 6.6$ Hz, $CHMe_2$), 1.35 (d, 6H, $J = 6.6$ Hz, $CHMe_2$), 1.31 (d, 6H, $J = 6.9$ Hz, $CHMe_2$), 1.19 (s, 3H, $N=C(Me)-CHH-N$), 0.86 (d, 6H, $J = 6.9$ Hz, $CHMe_2$). Anal. Calcd. for $C_{27}H_{39}N_2Cl_2Al$: C, 66.25; H, 8.03; N, 5.72. Found: C, 66.85; H, 8.05; N, 5.62.

Synthesis of (2). Di^iPPDAB (1.00 g, 2.66 mmol) was added slowly to a colorless solution of Me_2AlCl (2.66 mL, 2.66 mmol) in toluene (5 mL); the solution turned dark orange. The reaction was stirred for 14 h, during which time the reaction turned pale yellow. Yellow crystals were isolated by slow evaporation. The compound acquired a green tint of color over time in the drybox. The yield was essentially quantitative (1.25 g): mp $210\text{ }^\circ\text{C}$ decomposed, slight orange color at $230\text{ }^\circ\text{C}$ (orange liquid). 1H NMR (250 MHz, δ , in C_6D_6): 6.98–7.28 (m, 6H, (*i*-Pr) $_2C_6H_3$), 4.35 (d, 1H, $J = 23$ Hz, $N=C(Me)-CHH-N$), 4.20 (sept, 1H, $J = 7$ Hz, $CHMe_2$), 3.86 (d, 1H, $J = 23$ Hz, $N=C(Me)-CHH-N$), 3.53 (sept, 1H, $J = 7$ Hz, $CHMe_2$), 3.16 (sept, 1H, $J = 6$ Hz, $CHMe_2$), 3.00 (sept, 1H, $J = 7$ Hz, $CHMe_2$), 1.53 (d, 3H, $J = 7$ Hz, $CHMe_2$), 1.44 (d, 3H, $J = 6$ Hz, $CHMe_2$), 1.41 (d, 3H, $J = 7$ Hz, $CHMe_2$), 1.24 (s, 3H, $N=C(Me)-CHH-N$), 1.28 (d, 3H, $J = 6$ Hz, $CHMe_2$), 1.21 (d, 3H, $J = 6$ Hz, $CHMe_2$), 1.17 (d, 3H, $J = 7$ Hz, $CHMe_2$), 0.95 (d, 3H, $J = 7$ Hz, $CHMe_2$), 0.86 (d, 3H, $J = 7$ Hz, $CHMe_2$), -0.33 (s, 3H, $AlCH_3$). Anal. Calcd. for $C_{28}H_{42}N_2ClAl$: C, 71.69; H, 9.02; N, 5.97. Found: C, 71.42; H, 9.07; N, 5.96.

Synthesis of (3). Me^sDAB (0.500 g, 1.71 mmol) was added slowly to a colorless solution of Me_2AlCl (1.71 mL, 1.71 mmol) in toluene (4 mL); the solution turned dark orange. The reaction was stirred for 14 h; during this time the reaction turned pale yellow. Colorless crystals were isolated by slow evaporation of the solvent. Over time, compound 3 acquired an orange tint on the crystals. Yield: 73.7% (0.485 g), mp $183\text{--}185\text{ }^\circ\text{C}$. 1H NMR (250 MHz, δ , in CD_2Cl_2): 7.03 (s, 2H, $(Me)_3C_6H_2$), 6.92 (s, 2H, $(Me)_3C_6H_2$), 4.49 (d, 2H, $J = 24$ Hz, $N=C(Me)-CHH-N$), 4.26 (d, 2H, $J = 24$ Hz, $N=C(Me)-CHH-N$), 2.36 (s, 9H, $(2,4,6-(CH_3)_3C_6H_2)$), 2.32 (s, 3H, $(p-Me)_3C_6H_2$), 2.28 (s, 3H, $(o-Me)_3C_6H_2$), 2.17 (s, 3H, $(o-Me)_3C_6H_2$), 1.98 (s, 3H, $N=C(Me)-CHH-N$), -0.60 (s, 3H, $AlCH_3$). Anal. Calcd. for $C_{22}H_{30}N_2ClAl$: C, 68.65; H, 7.86; N, 7.28. Found: C, 68.68; H, 8.00; N, 7.38.

Synthesis of (4). ^{2,6}Me₂Ph^{DAB} (0.500 g, 1.89 mmol) was added slowly to a colorless solution of Me₂AlCl (1.89 mL, 1.89 mmol) in toluene (9 mL); the solution turned dark orange. The reaction was immediately placed in the freezer. Crystals were isolated via slow cooling at -20 °C. Yield: 59.3% (0.40 g). Crystals were clear with a yellow tint and appeared to be thermally unstable long-term. ¹H NMR (300 MHz, δ, in C₆D₆): 6.80–7.06 (m, 6H, (Me)₂C₆H₃), 4.01 (d, 1H, J = 25 Hz, N=C(Me)-CHH-N), 3.67 (d, 1H, J = 25 Hz, N=C(Me)-CHH-N), 2.52 (s, 6H, (o-Me)₂C₆H₃), 2.21 (s, 3H, (o-Me)₂C₆H₃), 1.86 (s, 3H, N=C(Me)-CHH-N), 0.97 (s, 3H, (o-Me)₂C₆H₃), -0.29 (s, 3H, AlCH₃). Anal. Calcd. for C₂₀H₂₆AlClN₂: C, 67.31; H, 7.34; N, 7.85. Found: C, 65.34; H, 7.76; N, 7.44.

Synthesis of (5). ^{DIPP}DAB (1.54 g, 4.09 mmol) was added slowly to a colorless solution of Me₃Al (0.296 g, 4.09 mmol) in toluene (5 mL); the solution turned red. The reaction was placed in a freezer at -20 °C. Yellow/orange crystals were isolated. Yield: 67.9% (1.25 g), mp 180–182 °C. ¹H NMR (250 MHz, δ, in C₆D₆): 7.10–7.40 (m, 6H, (i-Pr)₂C₆H₃), 4.37 (s, 2H, N=C(Me)-CHH-N), 3.63 (sept, 1H, J = 7 Hz, CHMe₂), 3.02 (sept, 1H, J = 7 Hz, CHMe₂), 1.33 (d, 12H, J = 7 Hz, CHMe₂), 1.19 (d, 12H, J = 7 Hz, CHMe₂), -0.86 (s, 3H, Al(CH₃)₂). Anal. Calcd. for C₂₉H₄₅N₂Al: C, 77.63; H, 10.11; N, 6.24. Found: C, 77.53; H, 10.13; N, 6.41.

Synthesis of (6). ^{DIPP}DAB(Me₂) (1.33 g, 3.29 mmol) was dissolved in toluene (5 mL). AlMe₃ (0.237 g, 3.29 mmol) was added slowly to give a yellow solution. The reaction was placed in the freezer at -20 °C. Yellow crystals were isolated. Yield: 65.7% (1.03 g), mp 180–182 °C. ¹H NMR (250 MHz, δ, in CDCl₃): 7.35–7.08 (m, 6H, (i-Pr)₂C₆H₃), 3.74 (sept, 2H, J = 7 Hz, CHMe₂), 3.03 (sept, 2H, J = 7 Hz, CHMe₂), 2.03 (s, 3H, N=C(Me)₂-C(Me)-N), 1.34 (s, 6H, N=C(Me)₂-C(Me)-N), 1.30 (d, 6H, J = 7 Hz, CHMe₂), 1.28 (d, 6H, J = 7 Hz, CHMe₂), 1.15 (d, 6H, J = 7 Hz, CHMe₂), 1.08 (d, 6H, J = 7 Hz, CHMe₂), -0.88 (s, 6H, Al(CH₃)₂). Anal. Calcd. for C₃₁H₄₉N₂Al: C, 78.10; H, 10.36; N, 5.88. Found: C, 78.41; H, 10.06; N, 6.01.

Synthesis of (7). GaCl₃ (0.468 g, 2.66 mmol) was dissolved in toluene (5 mL). ^{DIPP}DAB (1.00 g, 2.66 mmol) was slowly added. The reaction mixture turned dark red immediately. The reaction was stirred for 18 h. Dark orange crystals formed from the dark red solution via slow evaporation. Yield: 68.1% (1.00 g), mp 118–119 °C. ¹H NMR (300 MHz, δ, C₆D₆): 9.13 (d, J = 8.1 Hz, 1H, GaN=CH), 7.58 (d, J = 8.1 Hz, 1H, N=CH), 6.88–7.11 (overlapping m, C₆H₃), 3.08 (sept, J = 6.6 Hz, 2H, CHMe₂), 2.70 (sept, 6.9 Hz, 2H, CHMe₂), 1.27 (d, J = 6.6 Hz, 6H, CHMe), 0.89 (d, J = 6.9 Hz, 12H, CHMe₂), 0.82 (d, J = 6.9 Hz, 6H, CHMe₂). Anal. Calcd. for C₂₆H₃₆N₂Cl₃Ga: C, 56.50; H, 6.57; N, 5.07. Found: C, 56.98; H, 6.62; N, 5.08.

Synthesis of (8). GaCl₃ (0.23 g, 1.33 mmol) was dissolved in toluene (4 mL). ^{DIPP}DAB (0.25 g, 0.67 mmol) was slowly added. The reaction mixture turned dark red immediately, and a red precipitate formed within minutes. The reaction was stirred overnight at rt, and then the precipitate was isolated by filtration. Yield: 80.0% (0.39 g), mp 163–166 °C. ¹H NMR (300 MHz, δ, C₆D₆): 9.86 (s, 2H, N=CH), 6.87–6.99 (overlapping m, C₆H₃), 2.75 (sept, J = 6.6 Hz, 4H, CHMe₂), 1.15 (d, J = 6.6 Hz, 12H, CHMe₂), 1.10 (d, J = 6.6 Hz, 12H, CHMe₂). Anal. Calcd. for C₂₆H₃₆Cl₂N₂Ga₂: C, 42.85; H, 4.98; N, 3.84. Found: C, 42.36; H, 4.98; N, 4.04.

Synthesis of (9). ^{DIPP}DAB (0.50 g, 1.32 mmol) was added slowly to a colorless solution of MeGaCl₂ (0.21 g, 1.32 mmol) in 5 mL of toluene. The solution turned dark red instantaneously. The reaction was stirred for 18 h. Orange crystals were isolated via slow evaporation of the toluene. Yield: 71.8% (0.51 g), mp 124–125 °C. ¹H NMR (300 MHz, δ, C₆D₆): 9.32 (d, J = 8 Hz, 1H, GaN=CH), 7.60 (d, J = 8 Hz, 1H, N=CH), 6.87–7.09 (overlapping m, C₆H₃), 3.10 (sept, J = 7 Hz, 2H, CHMe₂), 2.72 (sept, J = 7 Hz, 2H, CHMe₂), 1.18 (d, J = 7 Hz, 6H, CHMe₂), 0.90 (d, J = 7 Hz, 12H, CHMe₂), 0.84 (d, J = 7 Hz, 6H, CHMe₂), -0.05 (s, 3H, GaMe). Anal. Calcd. for C₂₇H₃₉N₂Cl₂Ga: C, 60.93; H, 7.39; N, 5.26. Found: C, 60.89; H, 7.38; N, 5.24.

Synthesis of (10). ^{DIPP}DAB (0.19 g, 0.50 mmol) was added slowly to a solution of MeGaCl₂ (0.16 g, 1.0 mmol) in toluene (2 mL). The solution turned orange immediately, and a precipitate began to form within a few minutes. After stirring at rt for 30 min, the precipitate was isolated by filtration. X-ray-quality crystals were grown from the NMR

solution. Yield: 65.1% (0.23 g), mp -150 °C (dec). ¹H NMR (300 MHz, δ, in C₆D₆): 10.10 (s, 2H, N=CH), 6.86–6.94 (m, 6H, C₆H₃), 3.21 (sept, J = 7 Hz, 4H, CHMe₂), 1.21 (d, J = 7 Hz, 24H, CHMe), -0.14 (s, 6H, GaMe₂). Anal. Calcd. for C₂₈H₄₂N₂Cl₄Ga₂: C, 48.89; H, 6.15; N, 4.07. Found: C, 49.09; H, 6.23; N, 3.98.

Synthesis of (11). ^{Mes}DAB (0.500 g, 1.71 mmol) was added slowly to a colorless solution of Me₂GaCl (0.231 g, 1.71 mmol) in toluene (6 mL), and the solution turned dark orange. The reaction was immediately placed in the freezer. Orange block crystals were isolated at -20 °C. Yield: 69.8% (0.510 g), mp 87 °C (dec). ¹H NMR (250 MHz, δ, in CD₂Cl₂): 8.84 (d, 1H, J = 8.3 Hz, N=C(Me)-CHH-N), 7.61 (d, 1H, J = 8.3 Hz, N=C(Me)-CHH-N), 7.09–6.82 (m, 4H, (Me)₃C₆H₂), 2.38–1.97 (m, 18H, (Me)₃C₆H₂), -0.19 (s, 6H, Ga(CH₃)₂). Anal. Calcd. for C₂₂H₃₀N₂ClGa: C, 61.79; H, 7.07; N, 6.55. Found: C, 61.75; H, 7.24; N, 6.64.

Synthesis of (12). ^{DIPP}DAB (1.00 g, 2.66 mmol) was added slowly to a colorless solution of Me₂GaCl (0.360 g, 2.66 mmol) in 10 mL of toluene. The solution turned deep orange instantaneously. Over 12 h, the color of the solution became dark green, and rod-shaped yellow crystals of **1** began to form. The solution was cooled to -30 °C. Colorless, green, yellow, and orange crystals were isolated and washed with cold pentane after 12 h. The yield was essentially quantitative (1.35 g). mp 170 °C with decomposition to an orange solid. Continued heating to 210 °C leaves a red liquid which will solidify to a green solid at rt. ¹H NMR (250 MHz, δ, in C₆D₆): 6.98–7.27 (m, 6H, (i-Pr)₂C₆H₃), 4.57 (d, 1H, J = 23 Hz, N=C(Me)-CHH-N), 4.32 (sept, 1H, J = 7 Hz, CHMe₂), 3.88 (d, 1H, J = 23 Hz, N=C(Me)-CHH-N), 3.38 (sept, 1H, J = 6 Hz, CHMe₂), 3.20 (sept, 1H, J = 6 Hz, CHMe₂), 2.90 (sept, 1H, J = 7 Hz, CHMe₂), 1.52 (d, 3H, J = 6 Hz, CHMe₂), 1.48 (d, 3H, J = 6 Hz, CHMe₂), 1.45 (d, 3H, J = 7 Hz, CHMe₂), 1.25 (s, 3H, N=C(Me)-CHH-N), 1.25 (d, 3H, J = 7 Hz, CHMe₂), 1.24 (d, 3H, J = 6 Hz, CHMe₂), 1.16 (d, 3H, J = 7 Hz, CHMe₂), 0.98 (d, 3H, J = 7 Hz, CHMe₂), 0.86 (d, 3H, J = 6 Hz, CHMe₂), 0.01 (s, 3H, GaCH₃). Anal. Calcd. for C₂₈H₄₂N₂ClGa: C, 65.71; H, 8.27; N, 5.47. Found: C, 65.99; H, 8.46; N, 5.30.

Synthesis of (13). ^{DIPP}DAB (1.00 g, 2.66 mmol) was added slowly to a colorless solution of Me₃Ga (0.305 g, 2.66 mmol) in 6 mL of toluene. The solution turned orange instantaneously. The reaction was stirred for 18 h. Yellow crystals were isolated via slow evaporation in toluene. Yield was essentially quantitative (1.33 g). mp 136–138 °C. ¹H NMR (250 MHz, δ, in CD₂Cl₂): 6.95–7.40 (m, 6H, (i-Pr)₂C₆H₃), 4.49 (s, H, N=C(Me)-CHH-N), 3.62 (sept, 2H, J = 7 Hz, CHMe₂), 2.98 (sept, 2H, J = 7 Hz, CHMe₂), 1.93 (s, 3H, N=C(Me)-CHH-N), 1.31 (d, 12H, J = 7 Hz, CHMe₂), 1.18 (d, 12H, J = 7 Hz, CHMe₂), -0.43 (s, 3H, Ga(CH₃)₂). Anal. Calcd. for C₂₉H₄₅N₂ClGa: C, 70.88; H, 9.23; N, 5.70. Found: C, 70.93; H, 9.56; N, 5.75.

Synthesis of (14). ^{DIPP}DAB(Me₂) (0.500 g, 1.24 mmol) was dissolved in toluene (3 mL). GaMe₃ (0.142 g, 1.24 mmol) was added slowly. The reaction mixture turned yellow. The reaction was stirred for 3 h. Yellow crystals were isolated by slow evaporation of the toluene. Yield: 91.4% (0.587 g), mp 155–160 °C. ¹H NMR (250 MHz, δ, in C₆D₆): 7.30–7.00 (m, 6H, (i-Pr)₂C₆H₃), 3.92 (sept, 2H, J = 7 Hz, CHMe₂), 3.04 (sept, 2H, J = 7 Hz, CHMe₂), 1.40 (d, 6H, J = 7 Hz, CHMe₂), 1.37 (s, 3H, N=C(Me)₂-C(Me)-N), 1.28 (d, 6H, J = 7 Hz, CHMe₂), 1.25 (d, 6H, J = 7 Hz, CHMe₂), 1.20 (s, 6H, N=C(Me)₂-C(Me)-N), 0.97 (d, 6H, J = 7 Hz, CHMe₂), -0.07 (s, 6H, GaCH₃). Anal. Calcd. for C₃₁H₄₉N₂Ga: C, 71.68; H, 9.51; N, 5.39. Found: C, 71.65; H, 9.64; N, 5.32.

Synthesis of (15). ^{tBu}DAB (0.500 g, 2.97 mmol) was dissolved in toluene (3 mL). Me₂GaCl (0.402 g, 2.97 mmol) was slowly added. The reaction was exothermic. White crystals formed immediately from the dark orange solution. The white crystals redissolved into the solvent. The reaction was allowed to stir overnight. Orange crystals fell out of the solution as it became darker in color. The solution was allowed to slowly evaporate. The crystals were washed with cold pentane. Over time, the crystals obtained an orange tint. Yield: 48.4% overall, 96.7% based on Ga (0.430 g). ¹H NMR (250 MHz, δ, C₆D₆): 9.13 (s, 2H, N=CH-CH=N), 1.08 (s, 18H, C(CH₃)₃), 0.47 (s, 6H, (CH₃)₂Ga), -0.20 (s, 6H, (CH₃)₂GaCl₂). Anal. Calcd. for

C₁₄H₃₂N₂Cl₂Ga: C, 38.32; H, 7.35; N, 6.38. Found: C, 38.51; H, 7.50; N, 6.37.

Synthesis of (16). ^{chex}DAB (0.500 g, 2.27 mmol) was added slowly to a colorless solution of Me₂GaCl (0.622 g, 4.60 mmol) in toluene (5 mL) to give a light green colored solution, which was immediately placed in the freezer. White crystals were isolated at -20 °C. Yield: 79.6% (0.89 g). ¹H NMR (300 MHz, δ, C₆D₆): 9.19 (s, 2H, N=CH-CH=N), 3.67 (s, 2H, *ipso*-C₆H₁₁), 1.84 (br, 4H, C₆H₁₁), 1.43 (br, 4H, C₆H₁₁), 1.32 (br, 2H), 1.00–1.05 (overlapping m, 10H, C₆H₁₁), 0.49 (s, 6H GaMe₂), -0.17 (s, 6H, Cl₂GaMe₂). Elemental analysis was not obtained due to thermal sensitivity.

Crystallographic Studies. The crystals were coated with oil (Paratone-N) and were mounted on the nylon fiber of a CryoLoop (obtained from Hampton Research, U.S.A.) that had been previously attached to a metallic pin using epoxy. The data were collected at the temperatures indicated in the tables on a Bruker X8 Apex II diffractometer using monochromated Mo K α radiation ($\lambda = 0.71073$ Å). Cell parameters were initially retrieved using the APEX2 software¹² and refined with the APEX2 software, and the SAINT software was used for data reduction. The structures were solved using direct methods and refined with the full-matrix least-squares method on F^2 with SHELXTL.¹³ The non-hydrogen atoms were refined anisotropically. Hydrogen atoms were included at geometrically idealized positions and were not refined. The isotropic thermal parameters of the hydrogen atoms were fixed at 1.5U equiv. of parent atom for terminal methyl group hydrogens and 1.2U for all others. Positional disorders and/or symmetry-imposed partial occupancy was identified and modeled in **1**, **2**, **10**, and **13**. Disordered solvent in **8** was accounted for using SQUEEZE.¹⁴ All final crystallographic figures shown in this document were generated by Diamond, v. 3.2 g.¹⁵ Crystallographic data for all compounds are listed in Tables 1, 2, and 3; however, in the interest of journal space, several of the thermal ellipsoid plots for the compounds are shown only in the Supporting Information. Structures have been deposited into the Cambridge Crystallographic database under the following numbers: **1**, 870996; **2**, 661028; **3**, 661029; **4**, 661030; **5**, 661033 (for information); **6**, 661032; **7**, 661024; **8**, 870997; **9**, 661023; **10**, 870998; **11**, 661025; **12**, 661026 (for information); **13**, 661027; **14**, 661031; **15**, 661021; and **16**, 61020.

RESULTS AND DISCUSSION

Aromatic ^RDAB Ligands—Aluminum Complexes. In 1979, an initial report from van Koten et al. reported that the interaction of Me₃Al with various ^RDAB ligands (R = aromatic or alkyl groups) could produce a range of products that depended on the nature of the R groups substituted on the ^RDAB ligand.⁵ Briefly summarizing this seminal work, van Koten et al. showed that (a) large R groups tended to produce simple 1:1 Lewis acid–base complexes containing dative N→AlMe₃ bonds and (b) aromatic or smaller alkyl R groups tended to produce inserted products in which a methyl group migrated from AlMe₃ onto the ligand backbone, resulting in formal insertion of the C=N bond of the ligand into an Al–C bond. Products were identified and carefully characterized by ¹H and ¹³C NMR spectroscopy. As well, the authors noted that a unique rearrangement process was possible in the insertion reactions in which a ligand backbone hydrogen atom migrates to an adjacent carbon atom. It is of note that the R = 4-MeO(C₆H₄) and 4-MeC₆H₄ ^RDAB derivatives with AlMe₃ were later characterized by this group using single crystal X-ray diffraction and were definitively shown to have the inserted structures suggested by the initial NMR studies.¹⁶

As further background, Mair and co-workers reported that when AlCl₃ was used in place of methylated Al species with the ^{DIPP}DAB ligand that only Lewis acid–base adducts were formed and no inserted products were seen.¹⁷ Depending on reaction

Table 1. Crystallographic Data and Parameters for Aromatic-Substituted Al Complexes 1, 2, 3, 4, and 6

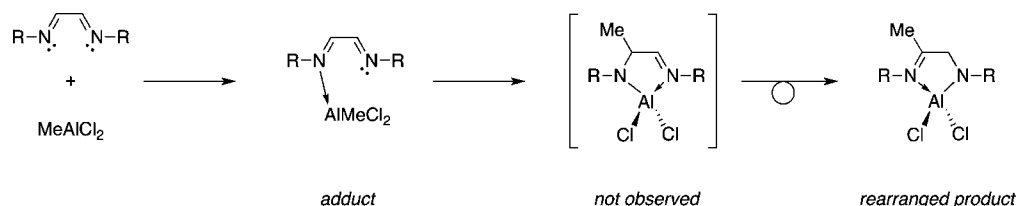
	1	2	3
empirical formula	C ₂₇ H ₃₉ AlCl ₂ N ₂	C ₂₈ H ₄₂ AlClN ₂	C ₂₂ H ₃₀ AlClN ₂
fw	489.48	469.07	384.91
T, K	172(2)	223(2)	223(2)
cryst size (mm)	0.31 × 0.24 × 0.15	0.30 × 0.30 × 0.20	0.30 × 0.10 × 0.10
cryst syst	orthorhombic	orthorhombic	triclinic
space group	<i>Pnma</i>	<i>Pnma</i>	<i>P1</i>
<i>a</i> , Å	12.2900(3)	12.4112(4)	8.2488(3)
<i>b</i> , Å	21.4033(6)	21.4045(7)	10.9973(4)
<i>c</i> , Å	10.5018(3)	10.5492(4)	13.3696(4)
α , deg	90.00	90.00	95.589(2)
β , deg	90.00	90.00	101.687(2)
γ , deg	90.00	90.00	107.113(2)
volume, Å ³	2762.46(13)	2802.45(17)	1119.01(7)
Z	4	4	2
calcd density, g/cm ³	1.177	1.112	1.142
μ (Mo K α), mm ⁻¹	0.284	0.185	0.218
R1 [$I > 2\sigma(I)$] ^a	0.0416	0.0506	0.0623
wR2 [$I > 2\sigma(I)$] ^b	0.1071	0.1243	0.1698
	4	6	
empirical formula	C ₂₀ H ₂₆ AlClN ₂	C ₃₁ H ₄₉ AlN ₂	
fw	356.86	476.70	
T, K	223(2)	223(2)	
cryst size (mm)	0.50 × 0.20 × 0.20	0.46 × 0.41 × 0.25	
cryst syst	triclinic	triclinic	
space group	<i>P1</i>	<i>P1</i>	
<i>a</i> , Å	8.3271(5)	8.4376(2)	
<i>b</i> , Å	10.0610(6)	9.7487(3)	
<i>c</i> , Å	13.4920(8)	19.3503(6)	
α , deg	77.792(3)	82.012(2)	
β , deg	78.412(4)	80.823(2)	
γ , deg	66.779(4)	69.652(2)	
volume, Å ³	1006.71(10)	1467.24(7)	
Z	2	2	
calcd density, g/cm ³	1.177	1.079	
μ (Mo K α), mm ⁻¹	0.237	0.089	
R1 [$I > 2\sigma(I)$] ^a	0.0569	0.0433	
wR2 [$I > 2\sigma(I)$] ^b	0.1503	0.1223	

$${}^a R_1 = \frac{\sum ||F_o| - |F_c||}{\sum |F_o|}, \quad {}^b wR_2 = \left\{ \frac{\sum [\omega(F_o^2 - F_c^2)]^2}{\sum [\omega(F_o^2)]^2} \right\}^{1/2}$$

stoichiometry, Mair could observe both 1:1 and 2:1 AlCl₃–^{DIPP}DAB complexes, and these were structurally characterized by X-ray crystallography. Quite interestingly, Mair was unable to prepare either the 1:1 or 2:1 adduct in the bulk as a pure substance, as mixtures of the two compounds were produced in all cases. However, single crystals of each adduct could be physically separated and isolated from the complex mixture.

In this report, we have investigated the interactions of aluminum and gallium species (Me_xMCl_{3-x}, $x = 0-3$, M = Al, Ga) with various aromatic and alkyl-substituted DAB ligands, expanding the range of both main-group starting compounds as well as the ^RDAB ligands. In this initial section, the interactions of methylated aluminum chlorides with aromatic ^RDAB ligands will be presented. Shown in Scheme 1 are the overall reactions for the preparation of these methylated Al complexes, keeping in mind that Mair had previously reported the interaction of

Scheme 2. Formation of Final Product 1 Indicating Initial Adduct Formation, Then Insertion Intermediate Compound (Not Observed), Followed by CH₃/H Rearrangement (from van Koten et al.⁵)



ligand and the specific methylated Al compound were slowly added together in a 1:1 molar ratio at room temperature under argon using toluene as a solvent. Depending on the final thermal sensitivity of each product, the reactions were stirred either overnight at room temperature or stored at the slightly lowered temperature of $-20\text{ }^{\circ}\text{C}$. In no case was external heating required, as good to essentially quantitative yields of the products were obtained without additional heating. The products **1–6** were isolated as X-ray quality crystalline solids.

When MeAlCl_2 is treated with the bulky ^{DIPP}DAB ligand in toluene solution at room temperature for less than 1 h followed by solvent removal, an oil was obtained whose ¹H NMR spectrum was consistent with a simple adduct; however, upon redissolution and storage in toluene at $-20\text{ }^{\circ}\text{C}$, this oil underwent further reaction to deposit analytically pure, colorless, X-ray quality crystals of **1**. Investigation of these crystals by ¹H and ¹³C NMR spectroscopy indicated that the final geometry in solution was not an adduct but rather a structure more consistent with an inserted and rearranged product. In subsequent syntheses of **1**, the immediately formed red solution was allowed to stir overnight, and **1** precipitated out as a white powder during that time. The oil was not isolated as only the final product was desired. The reaction sequence given in Scheme 2 is instructive and is based on the work of van Koten et al.⁵ This reaction indicates that the directly inserted product expected from C=N insertion into an Al–C bond after initial adduct formation is not observed. Rather, a subsequent rearrangement occurs where the H atom attached to the methylated carbon migrates to the other backbone carbon. This rearrangement reaction was briefly described in the Introduction and presented in more detail previously by van Koten et al. and as such does not require extensive discussion.⁵ However, it is important to note that the two possible inserted-product structures can be easily distinguished in solution by ¹H NMR spectroscopy, as the directly inserted complex contains a vinylic H proton and an allylic H proton that couple to each other, while the rearranged product contains two allylic protons and no vinylic protons. The ¹H NMR spectrum of **1** showed the presence of only allylic protons on the carbon backbone, characteristic of the rearranged product seen earlier by both van Koten et al. and us.^{4,5} However, in order to confirm the geometry of **1**, we performed a single-crystal X-ray analysis. **1** crystallized in the centrosymmetric space group *Pnma*, and the structure is shown in Figure 2. There is a crystallographic mirror plane through the Al(1) atom that bisects the five-membered ring. Therefore, the methyl group [C(14)] that has migrated can occupy either side of the diimine backbone and crystallographically shows half occupancy on either of the C(13) carbon atoms on the backbone. In Figure 2, only one of the possible structures is shown. Due to this crystallographic symmetry, it is impossible to distinguish between the two separate Al–N bonds (dative and covalent), as well as the

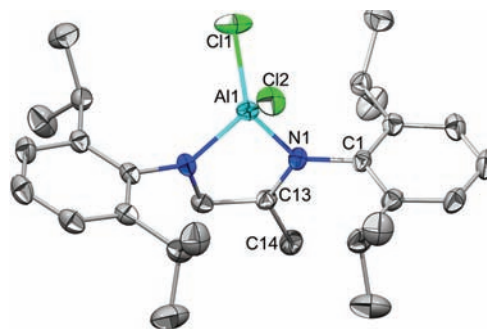


Figure 2. Molecular structure of **1** (50% ellipsoids). For clarity, hydrogen atoms are not shown. Due to symmetry, the Al(1)–N(1) bond is an average length of the expected Al–N_{dative} and Al–N_{covalent} bonds, and the N(1)–C(13) bond is an average of the expected C–N and C=N bonds. Selected bond lengths (Å) and angles (deg): Al(1)–Cl(1) = 2.1253(10), Al(1)–Cl(2) = 2.1146(10), Al(1)–N(1) = 1.8717(14), C(13)–N(1) = 1.368(2); Cl(1)–Al(1)–Cl(2) = 108.10(4), N(1)–Al(1)–N(1) = 87.27(9).

different C–N and the C=N bonds that are expected. The Al–N and C–N bond lengths that are observed and reported in Figure 2 are averages of the two separate values.

Progressing along the $\text{Me}_x\text{AlCl}_{3-x}$ ($x = 1-3$) series we next investigated the treatment of Me_2AlCl with a variety of substituted aromatic ^RDAB ligands. The ^RDAB ligand substituents chosen for study were the sterically bulky ^{DIPP}DAB ligand used above, the slightly less-bulky ^{Mes}DAB group, and the related ^{2,6Me2Ph}DAB group. The bulky ^{DIPP}DAB ligand reacted with Me_2AlCl in toluene at room temperature to give a dark orange solution that turned light yellow upon standing for 14 h. Slow evaporation of the solvent afforded **2** as analytically pure yellow crystals in essentially quantitative yield. Upon standing at room temperature over time, **2** developed a green tint and lost crystallinity; however, a satisfactory elemental analysis for **2** could be obtained. Storage at $-20\text{ }^{\circ}\text{C}$ suppressed formation of the green color. The ¹H NMR data for **2** suggested that the structure in solution was similar to its Ga analogue that we have previously reported (this mixed green/yellow crystalline compound is also briefly mentioned below as compound **12**)⁴ and to inserted/rearranged complexes prepared by van Koten et al.⁵

In order to confirm the identity of **2**, we performed a single crystal X-ray analysis on the isolated crystals, and the structure of **2** is shown in Figure 3. Compound **2** is structurally similar to our previously reported Ga analogue, and the thermal ellipsoid plot shows that the addition of ^{DIPP}DAB to Me_2AlCl results in the rearranged product shown in Scheme 2. While most of the metrical parameters for **2** are within the values expected and do not merit extensive discussion, we note that, like **1**, compound **2** crystallizes in space group *Pnma*, and as such there is a crystallographic mirror plane through the molecule. The migrated

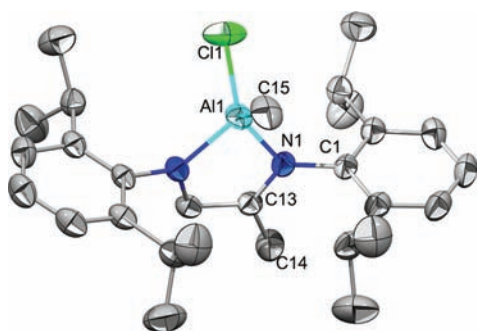


Figure 3. Molecular structure of **2** (50% ellipsoids). For clarity, hydrogen atoms are not shown. Due to symmetry, the Al(1)–N(1) bond is an average length of the expected Al–N_{dative} and Al–N_{covalent} bonds, and the N(1)–C(13) bond is an average of the expected C–N and C=N bonds. Selected bond lengths (Å) and angles (deg): Al(1)–Cl(1) = 2.097(4), Al(1)–C(15) = 2.01(2), Al(1)–N(1) = 1.8890(15); Cl(1)–Al(1)–C(15) = 112.7(7), Al(1)–N(1)–C(1) = 129.10(11), Al(1)–N(1)–C(13) = 112.78(12).

methyl group [C(14)] has 50% occupancy on each of the C(13) carbon atoms on the backbone, and Cl(1) and C(15) are disordered in a 65:35 ratio. The distinct differences in the amido/imido N–Al bonds could not be seen, nor could the differences in the C–N versus C=N bonds. In Figure 3, again only one of the two possible isomers is shown.

The reactions of Me₂AlCl with the slightly less-bulky ^{Mes}DAB and ^{2,6Me₂Ph}DAB ligands proceeded similarly to the reaction of ^{DIPP}DAB with Me₂AlCl. A room temperature reaction of ^{Mes}DAB and Me₂AlCl in toluene led to the eventual formation of compound **3**. Isolation via the gradual removal of solvent afforded analytically pure, X-ray quality crystals of **3** in 73.7% yield. ¹H NMR analysis of the colorless crystals of **3** in C₆D₆ indicated a solution geometry consistent with the rearranged structure seen also in **2**. Single crystal X-ray diffraction analysis confirmed the structure of **3** to be analogous to **2**, and the solid-state structure for **3** is shown in Figure 4. Unlike **2**, **3**

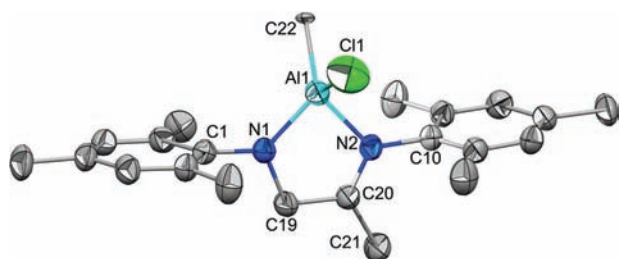


Figure 4. Molecular structure of **3** (50% ellipsoids). For clarity, hydrogen atoms are not shown. Selected bond lengths (Å) and angles (deg): Al(1)–N(1) = 1.817(3), Al(1)–N(2) = 1.970(3), Al(1)–C(22) = 2.004(3), Al(1)–Cl(1) = 2.1321(17), N(2)–C(20) = 1.286(4), N(1)–C(19) = 1.446(4); Cl(1)–Al(1)–C(22) = 108.45(10), N(1)–Al(1)–N(2) = 85.65(12), Al(1)–N(1)–C(19) = 114.9(2), Al(1)–N(2)–C(20) = 112.7(2).

crystallized in space group *P1* and as such did not possess a crystallographic plane of symmetry bisecting the five-membered ring. Therefore, individual bond lengths within the ring could be determined, and the unsymmetrical nature of the heterocyclic ring can thus be easily observed. There are two crystallographically distinct (but very similar) molecules in the unit cell of **3**, and as such we will only discuss one of them. The

differences in the Al(1)–N(1) [1.817(3) Å] and Al(1)–N(2) [1.970(3) Å] bond lengths inside the ring clearly show the distinctive changes between a typical N–Al single bond and an N→Al dative bond. As well, the two C–N bonds in the ring also demonstrate substantial differences in length—the N(2)–C(20) bond length of 1.286(4) Å is significantly shorter than the N(1)–C(19) bond length of 1.446(4) Å, thus indicating the double bond nature of N(2)–C(20) versus the single bond character of N(1)–C(19). The bond lengths in the ring are consistent with the rearranged structure shown in Scheme 2.

Multiple reactions of the ^{2,6Me₂Ph}DAB ligand with Me₂AlCl showed that the product **4** produced in a room temperature synthesis began to decompose upon storage at 25 °C. The single crystal X-ray structure of **4** indicated that the structure is very similar to **3**, space group *P1*, with distinctive bond lengths within the five-membered ring indicating the presence of discrete C–N, C=N, N–Al, and N→Al bonds within the ring, consistent with a rearranged product. There are two crystallographically distinct (but very similar) molecules in the unit cell of **4**. No other bond lengths or angles deserve any extended discussion. Due to the similarity of the structures of **3** and **4**, the thermal ellipsoid plot of **4** is not shown here. However, a structural diagram is available in the Supporting Information, and the structural details are given in Table 1.

As mentioned in the Introduction, most of the previous literature in this area had utilized Me₃Al as the main-group metal. ^RDAB ligands used prior to our work included variations in which R = 4-MeC₆H₄ or 4-(MeO)C₆H₄, both of which had been structurally characterized by van Koten et al. and shown to have the “rearranged product” structure.¹⁶ To complete the Me_xAlCl_{3-x} (*x* = 1–3) series using the ^{DIPP}DAB ligand, we also examined the interaction of Me₃Al with this ligand. The ^{DIPP}DAB ligand and Me₃Al were reacted at room temperature in toluene to form a red solution. Cooling to –20 °C afforded analytically pure, X-ray quality yellow-orange crystals of **5** in 67.9% isolated yield, and no thermal instability for **5** was observed. Analysis of the ¹H NMR data indicated that the solution structure was again the rearranged, five-membered ring product, consistent with the previous aryl-substituted Al complexes. We note that we had previously prepared this compound, characterized it by X-ray crystallography, and deposited the structure into the Cambridge Structural Database as a private communication (CCDC 661033). After our deposition, the structure of **5** was reported as part of a study by the Gibson group.¹⁸ While the exact preparation method differed as Gibson et al. used refluxing toluene for 12 h, the overall yields were similar and the structures virtually identical. As in **2** above, **5** crystallizes in the centrosymmetric space group *Pnma*, and as such the migrated methyl group has half-occupancy on each of the backbone carbon atoms. This plane of symmetry also enforces that the different Al–N and C–N bonds cannot be distinguished. As the structure of **5** was described previously by Gibson et al., it is not necessary to discuss it more fully. However, for completeness, a thermal ellipsoid plot of **5** is provided in the Supporting Information.

Last, for the aromatic ^RDAB ligand–aluminum complexes, we were interested in whether we could sterically block the migration of the methyl group from the Al atom onto the C–C backbone of the ^RDAB ligand. It was clear based on the work described above, as well as prior van Koten and Vrieze studies, that in cases of aryl-substituted DAB ligands the migration of a methyl group to the backbone always occurs, regardless of the size of the aromatic substituent, while the AlCl₃ experiments

from the Mair group indicate that chlorides do not migrate. We attached the sterically largest aromatic group—DiPP—onto a modified DAB ligand that contained a dimethylated rather than a diprotio backbone (Scheme 1). $\text{DiPPDAB}(\text{Me}_2)$ and Me_3Al were reacted slowly at room temperature in toluene, and the product was allowed to crystallize at -20°C . Yellow, analytically pure crystals were produced in 65.7% yield. ^1H NMR analysis indicated the presence of an $-\text{AlMe}_2$ moiety, as well as a singlet integrating on two Me groups on the diimine backbone and a singlet integrating to a single Me group on the backbone. Thus, the NMR integration data were strongly suggestive that product **6** was not the Lewis acid–base adduct as would be expected if no methyl migration had taken place. For confirmation, we performed a single crystal X-ray structural analysis on **6**. Compound **6** crystallizes in space group $P\bar{1}$, and the structure is shown in Figure 5. Again, the

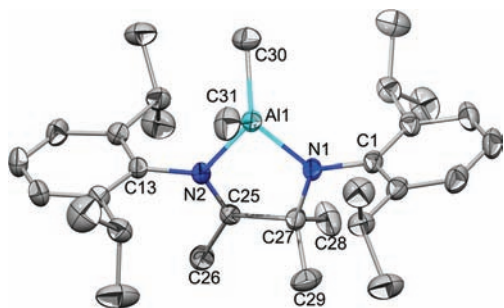


Figure 5. Molecular structure of **6** (50% ellipsoids). For clarity, hydrogen atoms are not shown. Selected bond lengths (Å) and angles (deg): $\text{Al}(1)\text{--N}(1) = 1.8471(9)$, $\text{Al}(1)\text{--N}(2) = 1.9875(10)$, $\text{Al}(1)\text{--C}(30) = 1.9680(15)$, $\text{Al}(1)\text{--C}(31) = 1.9648(15)$, $\text{N}(2)\text{--C}(25) = 1.2865(14)$, $\text{N}(1)\text{--C}(27) = 1.4682(14)$; $\text{C}(30)\text{--Al}(1)\text{--C}(31) = 108.48(7)$, $\text{N}(1)\text{--Al}(1)\text{--N}(2) = 84.40(4)$.

$\text{N}(1)\text{--Al}(1)$ amido single bond is significantly shorter than the $\text{N}(2)\rightarrow\text{Al}(1)$ dative bond, and the $\text{C}(25)\text{--N}(2)$ double bond is much shorter and distinct from the $\text{C}(27)\text{--N}(1)$ single bond. It is apparent that the presence of methyl groups on the backbone prior to reaction is not sufficient to keep the $\text{Al}\text{--Me}$ groups from migrating onto the diimine backbone, as the migrated methyl group can be clearly seen as one of the two methyl groups on $\text{C}(27)$ versus the single methyl group attached to $\text{C}(25)$.¹⁹

Aromatic R^{DAB} Ligands—Gallium Complexes. As one might suspect, analogous reactions utilizing methylated gallium compounds with aromatic R^{DAB} ligands are significantly less studied than their aluminum counterparts and appear to be limited to our previous report dealing with the multichromic crystals produced from the interaction of Me_2GaCl with the DiPPDAB ligand.⁴ We do note, however, that related compounds of lower-valent Ga^{I} –diimine adducts have been well-documented in particular by the group of Jones,²⁰ but they do not fall into the scope of our higher-valent Ga^{III} interests. Again utilizing primarily the DiPPDAB ligand, we investigated the interactions of aromatic-substituted R^{DAB} ligands with GaCl_3 , MeGaCl_2 , Me_2GaCl , and Me_3Ga . Shown in Scheme 3 are the reactions that will be discussed in this section, leading to either adduct products, inserted and rearranged products, or surprisingly a cation/anion pair.

Treatment of the DiPPDAB ligand in toluene at room temperature for 18 h with a 1:1 ratio of GaCl_3 afforded the monoadduct **7** in which GaCl_3 has coordinated to one of the backbone nitrogen atoms. After removal of the toluene from

the deep red solution, the monoadduct **7** was isolated in 68.1% yield as dark orange crystals. The ^1H NMR data indicated that the molecule had an unsymmetrical structure in solution, thus indicating a monoadduct, but the solution also showed the presence of free DiPPDAB ligand. The presence of the ligand in solution was confirmed by an NMR tube experiment in which a 50% excess of ligand was added to the reaction mixture, and the resonances due to the free ligand increased by 50%. The observed unsymmetrical structure by NMR was somewhat unexpected by us based on prior literature. A symmetric structure would be consistent with either a 1:1 complex of $\text{GaCl}_3/\text{DiPPDAB}$ ligand in which DiPPDAB is chelated symmetrically to GaCl_3 or a situation in which the GaCl_3 is rapidly migrating between the two N atoms, thus equivalencing the two halves of the molecule on the NMR time scale. van Koten et al. had noted that, in the case of AlMe_3 and R^{DAB} , rapid exchange occurred even at -90°C in toluene,⁵ and so we were expecting a symmetric structure in the NMR spectrum. As well, Mair et al. had seen in the AlCl_3 case with DiPPDAB the presence of both mono- and diadducts of AlCl_3 with the ligand in solution.¹⁷ We did not observe any peaks in the NMR spectrum that could be assigned to a symmetrical complex.

Compound **7** crystallized in the space group $P2(1)/c$, and the molecular geometry is shown in Figure 6. The solid-state structure of **7** is a monoadduct in which only the E/E isomer is found, in contrast to Mair et al. who observed formation of both the E/E and E/Z isomers for the $\text{AlCl}_3/\text{DiPPDAB}$ monoadduct.¹⁷ The structure resembles that found for the free ligand, with the obvious addition of the GaCl_3 fragment complexed to one N atom. There are two slightly different molecules in the unit cell, and only one of them is shown in Figure 6. There are negligible differences in bond lengths between these two independent molecules, and only slight differences are found in the bond angles. If one looks at the asymmetric unit, one Ga is bound to the “left” nitrogen atom, and the other is bound to the “right” nitrogen atom. In a packing diagram, this has the effect of causing each layer of molecules to have the GaCl_3 unit pointing in the opposite directions. As was seen previously in the AlCl_3 case,¹⁷ the conjugation of the diimine backbone is largely unaffected by the presence of the GaCl_3 , as the $\text{C}=\text{N}$ bond lengths are identical in length.

The preparation of the 2:1 $\text{GaCl}_3/\text{DiPPDAB}$ complex **8** followed a similar route to the preparation of **7** except with the change in molar ratio. The solution again turned dark red immediately, and a red precipitate was formed within minutes. After stirring overnight at room temperature, product **8** was isolated in 80% yield by filtration as an analytically pure powder. Cooling of the supernatant afforded X-ray quality crystals of **8**. The ^1H NMR spectral data for the deposited powder and the isolated crystals were identical and indicated the presence of a vinyl proton at 9.86 ppm. As we had also seen with **7**, free DiPPDAB ligand was also present in the spectra. This indicated to us that we had an entirely different solution geometry with **8** than with the other complexes, and so an X-ray diffraction analysis was performed on **8**.

The structure shown in Figure 7 is quite different from the previous structures seen by either van Koten et al., Mair et al., or us. **8** crystallizes in space group $P2(1)/c$ and consists of a discrete cation/anion pair. The bond lengths and angles found in **8** are similar to those found in the cation/anion pair reaction product of an alkyl-substituted diimine ($^{\text{tBu}}\text{DAB}$) with 2 mol of GaCl_3 that was previously reported by Cowley et al., as well as a

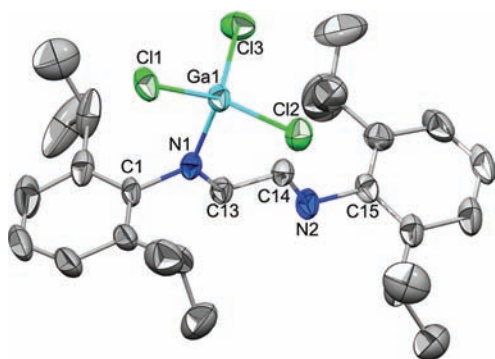
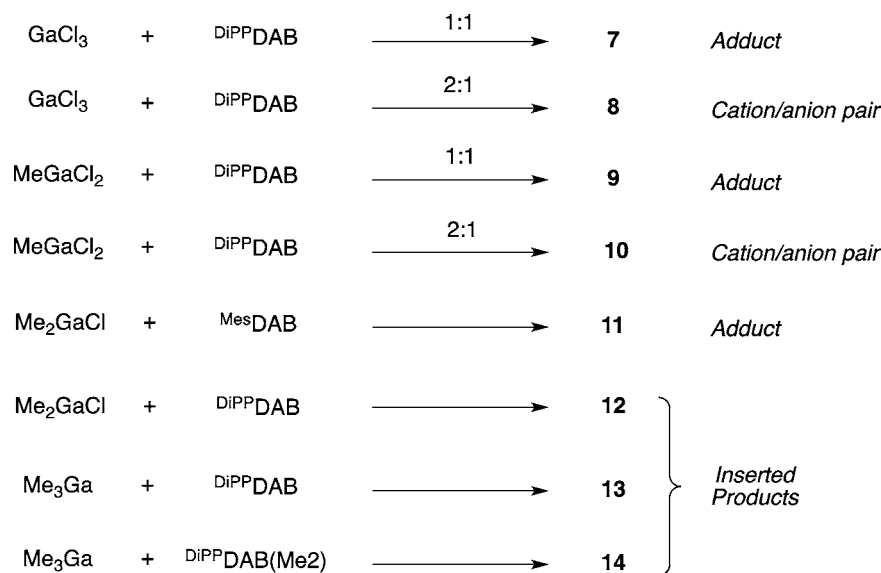
Scheme 3. Outline for Products of Gallium Species and ^RDAB Ligands (R = Aromatic)

Figure 6. Molecular structure of **7** (50% ellipsoids). For clarity, hydrogen atoms are not shown. Selected bond lengths (Å) and angles (deg): Ga(1)–N(1) = 2.021(3), N(1)–C(13) = 1.278(4), C(13)–C(14) = 1.472(5), C(14)–N(2) = 1.268(5), N(2)–C(15) = 1.432(5), N(1)–C(1) = 1.470(5); C(1)–N(1)–Ga(1) = 118.7(2), C(1)–N(1)–C(13) = 115.3(3), Ga(1)–N(1)–C(13) = 126.0(3).

BIAN-complex of $[\text{GaCl}_2]^+$ from the Clyburne group.²¹ In both cases, there is found an acute N–Ga–N bite angle of ~ 83 – 84° , and the bond lengths present in both products are consistent with those shown in Scheme 4. The structure of **8** is also consistent with an initial reaction of the DiPPDAB ligand to coordinate (or possibly chelate) to a molecule of GaCl₃, followed by a reaction with a second molecule of GaCl₃ that acts as a halide abstractor to form the $[\text{GaCl}_4]^-$ anion (Scheme 4). We have no evidence by either NMR or X-ray data that a dicoordinated adduct, as reported by Mair et al. for the 2:1 Al analogue,¹⁷ is ever formed. This result may show the subtle differences in reactivity patterns exhibited by Al versus Ga.

Interaction of the DiPPDAB ligand in a 1:1 ratio with MeGaCl₂ in toluene at room temperature for 18 h gave a deep red solution from which dark orange crystals of **9** could be

isolated in 71.8% yield upon the slow removal of solvent. A ¹H NMR spectrum taken of the orange crystals indicated that a coordination adduct had formed rather than the ultimate inserted/rearranged product found in the Al analogue **1**; however, recall that an adduct was initially observed during the preparation of **1** as well as an unstable intermediate. The ¹H NMR of **9** showed a pattern typical of unsymmetrical binding to the DiPPDAB ligand in which only one N atom is coordinated. As with **7** and **8**, free DiPPDAB ligand was also observed in the ¹H NMR spectrum. The thermal ellipsoid plot of **9** is shown in the Supporting Information, as the solid-state structure of **9** is similar to that of the adduct **7** using GaCl₃ and the *E/E* isomer of the AlCl₃ adduct reported by Mair et al. N(1) has the expected trigonal geometry ($\sum_{\text{bond angles}} \text{N}(1) = 359.96^\circ$), and the N(1)–C(26) bond length (1.281(4) Å) is very slightly elongated relative to the N(2)–C(25) bond length (1.256(4) Å).

As free DiPPDAB ligand was observed in the reaction solution during preparation of **9**, it was of interest to add more MeGaCl₂ to attempt to push the reaction toward completion. We next added a 2:1 ratio of MeGaCl₂ relative to DiPPDAB ligand under similar reaction conditions. The solution turned orange immediately upon addition, and an orange precipitate began forming within minutes. After 30 min, the precipitate was collected by filtration in 65.1% yield (after identification). The ¹H NMR spectrum of **10** indicated the presence of vinyl protons on the DAB backbone, and no allylic proton resonances, indicating a symmetric structure in solution. As well, only a single upfield resonance was present in the GaCH₃ region that integrated for one GaCH₃ per backbone vinyl proton. On the basis of the ¹H NMR spectrum, one would likely expect the symmetric structure of **10** to arise from a dicoordinated adduct of MeGaCl₂ with the DiPPDAB ligand. However, as we saw above in the 2:1 GaCl₃ case to produce **8**, a

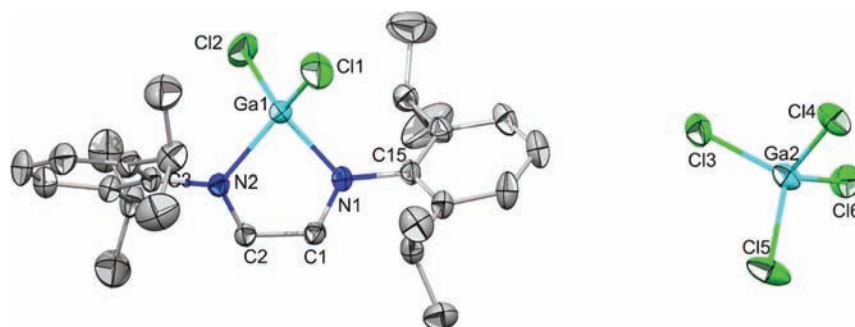
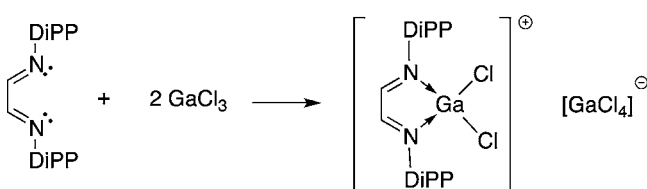


Figure 7. Molecular structure of **8** (50% ellipsoids). For clarity, hydrogen atoms are not shown. Selected bond lengths (Å) and angles (deg): Ga(1)–N(1) = 1.983(3), Ga(1)–N(2) = 2.005(3), N(1)–C(1) = 1.277(5), N(2)–C(2) = 1.283(5), C(1)–C(2) = 1.478(5); N(1)–Ga(1)–N(2) = 83.56(13), Ga(1)–N(1)–C(1) = 111.2(3), Ga(1)–N(2)–C(2) = 109.6(3).

Scheme 4. Reaction of ^{DiPP}DAB Ligand and GaCl₃ to Yield **8**



dicoordinated adduct was not seen, but rather another cation/anion pair was formed. In the case of **10**, however, the expected cation/anion pair would be [(^{DiPP}DAB)GaMeCl]⁺ [MeGaCl₃][−], which could give a symmetrical ¹H NMR pattern for the cation, but not a single –GaCH₃ resonance. In order to confirm the structure of **10**, we grew X-ray quality crystals from the NMR tube. The structure obtained (Figure 8) was a cation/anion pair. The most reasonable solution to the crystal structure was obtained with a [GaCl₄][−] anion and a [(^{DiPP}DAB)GaMeCl]⁺ cation in which the Cl and Me were each disordered over two positions in a roughly 55:45 ratio. We note that this does not correspond to the reaction stoichiometry nor the NMR data. The cation/anion pair that would best fit the NMR spectrum is [(^{DiPP}DAB)GaMe₂]⁺ [GaCl₄][−], which would result from disproportionation of the MeGaCl₂ starting material and is consistent with the elemental analysis. Also possible would be [(^{DiPP}DAB)GaMeCl]⁺ [MeGaCl₃][−] resulting from simple chloride abstraction as seen in **8**. Attempts to model each of these, however, were unsatisfactory. Problems with partial occupancy of Me and Cl in cation/anion pairs were also encountered in the reaction of Me₂AlCl with ^{tBu}DAB (vide infra).

As MeGaCl₂ yields an adduct **9** and the cation/anion pair **10** rather than inserted/rearranged products, these results indicate that MeGaCl₂ is more similar in behavior to AlCl₃ and GaCl₃ than to the dimethylated species Me₂MCl (M = Al, Ga) when treated with the bulky ^{DiPP}DAB ligand. The energetic drive to insert the C=N bond of the aromatic-substituted diimine into the Ga–CH₃ bond does not appear to be sufficient if only one methyl group is present on the central Ga atom, despite the fact that the Al analogue **1** does eventually produce an inserted/rearranged product (Figure 2).

Changing the aromatic ^RDAB ligand from ^{DiPP}DAB to a smaller ^{Mes}DAB ligand and changing the gallium species to Me₂GaCl surprisingly did not afford an inserted/rearranged product with Me₂GaCl, but rather again an adduct. Reaction of ^{Mes}DAB with Me₂GaCl in toluene immediately gave a vivid dark orange color in solution, and after stirring briefly at room

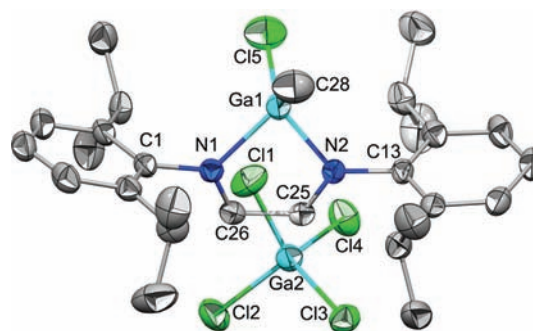
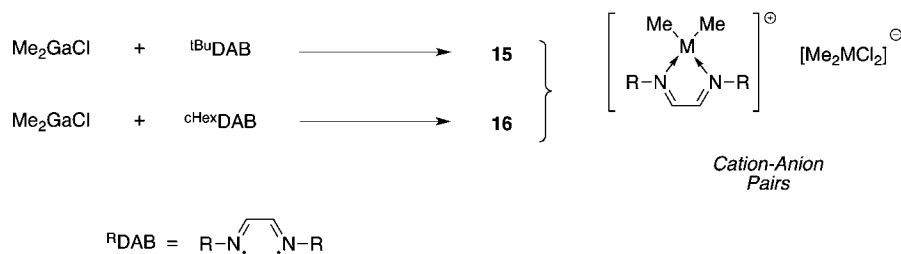


Figure 8. Molecular structure of **10** (50% ellipsoids). For clarity, hydrogen atoms are not shown. Selected bond lengths (Å) and angles (deg): Ga(1)–C(28) = 1.931(13), Ga(1)–Cl(5) = 2.023(3), Ga(1)–N(1) = 2.043(3), Ga(1)–N(2) = 2.037(3); Cl(5)–Ga(1)–C(28) = 116.9(4), N(1)–Ga(1)–N(2) = 80.13(12).

temperature the reaction mixture was cooled to –20 °C and stored. Dark orange, analytically pure crystals of **11** were isolated in 69.8% yield. ¹H NMR data were consistent with the solution structure of **11** as an adduct, and the X-ray structure of **11** confirmed the NMR assignment (shown in the Supporting Information and crystallographic data in Table 2). The solid-state structure is very similar to the other monoadducts discussed earlier and so no further discussion of the structure is needed. However, we do note that the only isomer present in the structure was the *E/E* isomer with no trace of the *E/Z* isomer found.

Interaction of Me₂GaCl with ^{DiPP}DAB to give **12** has been reported previously by us,⁴ although the preparation and analytical characterization are included here for completeness. The solid-state structure is the inserted/rearranged product (vide supra). Quite interestingly, identical crystal structures were obtained for **12** for yellow, green, or mixed yellow/green single crystals. The variation in color seen for crystals of **12** was attributed to the decomposition of a small amount of **12** to form trace levels of a highly colored blue compound that was present in the yellow crystals of **12**. While intensely colored solutions and products were prepared in this current study of methylated Al and Ga species with aromatic DAB ligands, it is noteworthy that none of the crystalline solids prepared demonstrated the multichromic behavior shown by **12**. Detailed characterization data for **12** have been published elsewhere;⁴ however, for completeness, the thermal ellipsoid plot of **12** is also shown in the Supporting Information. We note that we have also previously reported that if 2 equiv of

Scheme 5. Outline for Products of Me_2GaCl Reactions with Alkyl^RDAB Ligands

Me_2GaCl are treated with $\text{Di}^{\text{DIP}}\text{DAB}$ at low temperatures ($-30\text{ }^{\circ}\text{C}$), a diadduct is formed in low yields that was characterized by X-ray crystallography.⁴ This product is consistent with the Mair et al. results¹⁷ but different from our results with **8** and **10**. This diadduct converts to **12** upon warming to room temperature in solution, again inconsistent with the behaviors of **8** and **10**, which are both stable in solution.

In a similar preparative route to the other reactions above, changing the main group species to Me_3Ga and using the $\text{Di}^{\text{DIP}}\text{DAB}$ ligand afforded **13** in essentially quantitative yield. The reaction was allowed to stir at room temperature for 18 h in toluene, and concentration of the orange solution by gradual removal of toluene gave **13** as analytically pure, yellow crystals. Analysis of the ^1H NMR spectrum indicated that, as with **12**, the structure in solution was of the inserted/rearranged type. In this case, the integrated ratio of protons in the $-\text{GaMe}_2$ moiety versus the backbone $-\text{CH}_3$ group was important in rationalizing the solution structure, along with the absence of vinyl protons. The solid-state structure was confirmed by single crystal X-ray diffraction. Briefly, **13** crystallized in the centrosymmetric space group $Pnma$ and as such had a mirror plane of symmetry through the GaMe_2 group as well as bisecting the five-membered ring. Thus, individual C–N versus C=N bonds could not be distinguished. As this structure was very similar to others presented above, the thermal ellipsoid plot of **13** is presented only in the Supporting Information.

When GaMe_3 is treated with the dimethylated backbone diimine $\text{Di}^{\text{DIP}}\text{DAB}(\text{Me}_2)$ in toluene at room temperature for 3 h, **14** can be isolated in excellent yield (91.4%) as analytically pure, yellow crystals upon slow removal of the solvent. As with the Al analogue **6**, ^1H NMR spectral evidence indicated that the $\text{Di}^{\text{DIP}}\text{DAB}$ ligand had inserted into a Ga–Me bond of the GaMe_3 molecule and then undergone rearrangement. As in **6**, addition of the two methyl groups on the backbone of a sterically crowded R^{DAB} ligand is not capable of blocking the insertion process and forcing an adduct to be formed. The solid-state structure was determined by X-ray diffraction and showed that the structures in the solid and solution were consistent. Unlike **13**, **14** did not crystallize in a centrosymmetric space group, thus allowing the individual Ga(1)–N(1), Ga(1)–N(2), N(1)–C(26), and N(2)–C(25) bond lengths to be distinguished. The thermal ellipsoid plot for **14** is shown in the Supporting Information, while the important crystallographic data are given in Table 2.

Aliphatic R^{DAB} Ligands—Gallium and Aluminum Complexes. In order to serve as comparison molecules, we were interested in utilizing the more electron-rich, stronger-donating alkyl-substituted RDAB ligands¹⁰ in place of the various aromatic groups used earlier. Rather than exploring all possible permutations, it was decided to examine only a small subset of possible combinations, as we had seen above that only

a limited number of structural motifs were formed using aromatic RDAB ligands. As the work described above had in some cases involved Me_2GaCl and had given inserted/rearranged products instead of simple adducts, we chose to examine this main group species with both the *t*-butyl-substituted tBuDAB ligand and the cyclohexyl-substituted cHexDAB ligand (Scheme 5) to see if this reactivity trend continued.

Initial experiments involved the treatment of Me_2GaCl with the tBu^{DAB} ligand. A similar experimental procedure to those described above was followed, utilizing a 1:1 Ga/ tBu^{DAB} ligand ratio in toluene. In this case, the reaction was somewhat exothermic. White crystals formed immediately from the dark orange solution that gradually redissolved into the solvent. The reaction was allowed to stir overnight. Orange crystals precipitated from solution as the solution became darker in color upon gradual removal of the solvent. The isolated crystals were washed with cold pentane, giving **15** in essentially quantitative yield (based on Ga) in analytically pure form. The ^1H NMR analysis indicated that the structure was a cation/anion pair similar to what we had seen for **8** and **10**, and this solution structure was confirmed by X-ray diffraction (Figure 9). **15** crystallized in space group $P\bar{1}$, and the structure

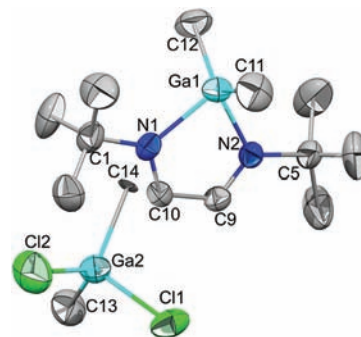


Figure 9. Molecular structure of **15** (50% ellipsoids). For clarity, hydrogen atoms are not shown. Selected bond lengths (Å) and angles (deg): Ga(1)–N(1) = 2.044(3), Ga(1)–N(2) = 2.054(3), C(10)–N(1) = 1.263(5), C(9)–N(2) = 1.258(5); N(1)–Ga(1)–N(2) = 80.80(12).

indicated that the discrete cation and anion pairs were well-separated and had no interionic contacts. Although there is no strict plane of symmetry bisecting the five-membered ring, there is a virtual plane of symmetry as the Ga(1)–N(2) and Ga(1)–N(1) bond distances are virtually identical (2.054(3) and 2.040(3) Å, respectively) and the N(1)–C(10) and N(2)–C(9) bond distances are also identical (1.263(5) and 1.258(5) Å, respectively). As mentioned previously, Cowley et al. have reported a structurally characterized $[\text{GaCl}_2]^+$ cation containing a tBu^{DAB} ligand that also has two σ -bound N donor atoms, formed

when 2 equiv of GaCl_3 were treated with the $^{\text{tBu}}\text{DAB}$ ligand.^{21a} We note that the $\text{N}(6)\text{--Ga}(2)\text{--N}(7)$ angle in **15** is slightly more acute than what is observed in the Cowley et al. compound or in **8** ($80.80(12)^\circ$ for **15** versus $84.4(4)^\circ$ for Cowley et al. and $83.56(13)$ for **8**), and the $\text{Ga}\text{--N}$ bonds found in **15** are slightly longer as well.

Me_2GaCl was treated in a similar fashion with the less-hindered $^{\text{cHex}}\text{DAB}$ ligand. A 1:1 ratio of $\text{Ga}/^{\text{cHex}}\text{DAB}$ ligand produced a light green solution that was immediately placed in the freezer. White crystals of **16** were isolated at -20°C . Upon standing in the freezer, the crystals slowly acquired an orange color and appeared to be unstable at room temperature. The isolated yield of **16** was 79.6% when an optimal 2:1 $\text{Ga}/\text{diimine}$ ratio was used (after identification of the product). Like the previous $^{\text{Alkyl}}\text{DAB}$ derivative **15**, both the ^1H NMR data as well as the X-ray structure of **16** were consistent with the structural assignment as a cation/anion pair. **16** crystallized in space group $P\bar{1}$, which allowed for all of the various discrete bond lengths in the heterocycle to be determined (structure shown in the Supporting Information). Similarly to **15**, there was a virtual plane of symmetry bisecting the five-membered ring due to the virtually identical bond lengths of $\text{Ga}(1)\text{--N}(1)$ and $\text{Ga}(1)\text{--N}(2)$ and of $\text{N}(2)\text{--C}(1)$ and $\text{N}(1)\text{--C}(2)$, respectively. The bond lengths and angles around the central Ga atom were not remarkable relative to **15** and as such do not warrant detailed comments.

Last, we note that we also examined the interactions of Me_2AlCl with the $^{\text{tBu}}\text{DAB}$ ligand. Quite interestingly, and very unexpectedly based on our other results, the reactions using Me_2AlCl were quite inconsistent and irreproducible from experiment to experiment. Reactions performed under seemingly identical conditions gave completely different isolated products. We have performed these experiments using purchased Me_2AlCl obtained in hexane solution, as well as freshly prepared solid Me_2AlCl prepared from Me_3Al and AlCl_3 . We have obtained crystalline material in all cases, but the various structures obtained do not appear to correlate with any known preparative variable. It did appear, however, that the majority of the $\text{Me}_2\text{AlCl}/^{\text{tBu}}\text{DAB}$ experiments gave cation/anion pairs. However, the anionic fragment of the molecules, which would be expected to be the $[\text{Me}_2\text{AlCl}_2]^-$ anion after chloride abstraction with Me_2AlCl , was found in only some of the structures. The $[\text{MeAlCl}_3]^-$ anion was also found via crystallography, thus implying that some type of methyl/halide exchange was occurring in solution. This dynamic behavior is similar to the MeGaCl_2 case mentioned above that complicates the crystallographic identification of **10**. Aluminum alkyls and halides are known to redistribute in solution and can be used deliberately in a preparative sense, and so this complicating reaction must be occurring at a rate that is proving to be synthetically confounding. Attempts to understand this ill-behaved chemistry are currently underway.

SUMMARY

In this report, we have shown that $\text{Me}_x\text{MCl}_{3-x}$ ($x = 0\text{--}3$, $\text{M} = \text{Al}, \text{Ga}$) react with various aromatic and alkyl-substituted $^{\text{R}}\text{DAB}$ ligands give a variety of structures in solution and in the solid state. When combined with other related structures previously published in the literature, general trends of reactivity of these species can be deduced, although there are still some unexplained modes of reactivity. All methylated aluminum species react with aromatic-substituted $^{\text{R}}\text{DAB}$ ligands to provide final products that result from insertion and rearrangement

reactions. The addition of methyl groups onto the backbone of the $^{\text{R}}\text{DAB}$ ligand is insufficient to stop the insertion and migration process from occurring. In the case of MeAlCl_2 with $^{\text{DipP}}\text{DAB}$, the reaction could be followed spectroscopically from the monoadduct through the inserted/rearranged final product. Methylated gallium species, however, are much less predictable in their behavior with aromatic-substituted $^{\text{R}}\text{DAB}$ ligands. Depending on the exact species used, coordinated adducts can be formed and identified, or inserted/rearranged products similar to the aluminum reactions can be obtained. Quite interesting, cation/anion pairs were formed in which GaCl_3 or MeGaCl_2 acted as chloride acceptors, in stark contrast to the analogous Al reaction which formed either a dicoordinated adduct or an inserted/rearranged product. When alkyl-substituted $^{\text{R}}\text{DAB}$ ligands were used with Me_2GaCl , only cation/anion pairs were obtained. Unfortunately, when the same reactions were performed using Me_2AlCl as a reagent, only irreproducible results were obtained. The multicolored nature exhibited by single crystals of **12** was not found in any other compound, thus indicating that **12** appears to be unique in its ability to form yellow, green, and mixed yellow-green single crystals.

ASSOCIATED CONTENT

Supporting Information

Crystallographic data in CIF format for compounds **1**–**4**, **6**–**11**, and **13**–**16** and thermal ellipsoid plots of compounds **4**, **5**, **9**, **11**–**14**, and **16**. This material is available free of charge via the Internet at <http://pubs.acs.org>.

AUTHOR INFORMATION

Corresponding Author

*E-mail: rakemp@unm.edu.

Notes

The authors declare no competing financial interest.

ACKNOWLEDGMENTS

This work was financially supported by the National Science Foundation (Grant CHE09-11110 to R.A.K.), and the Laboratory Directed Research and Development Program at Sandia National Laboratories (LDRD 69940). D.A.D. was financially supported by the Natural Sciences and Engineering Research Council (NSERC) of Canada by means of a Postdoctoral Fellowship. The Bruker X-ray diffractometer was purchased via a National Science Foundation CRIF:MU award to the University of New Mexico (CHE04-43580), and the NMR spectrometers were upgraded via grants from the NSF (CHE08-40523 and CHE09-46690). Dr. Michael Katz (Northwestern University) provided valuable assistance with the X-ray crystallographic analysis of **10**. Sandia National Laboratories is a multiprogram laboratory managed and operated by Sandia Corporation, a wholly owned subsidiary of Lockheed Martin Corporation, for the U.S. Department of Energy's National Nuclear Security Administration under contract DE-AC04-94AL85000.

REFERENCES

- (1) (a) Johnson, L. K.; Killian, C. M.; Brookhart, M. *J. Am. Chem. Soc.* **1995**, *117*, 6414. (b) Small, B. L.; Brookhart, M.; Bennett, A. M. *J. Am. Chem. Soc.* **1998**, *120*, 4049. (c) Svejda, S. A.; Brookhart, M. *Organometallics* **1999**, *18*, 65. (d) Donski, G. J.; Rose, J. M.; Coates, G. W.; Bolig, A. D.; Brookhart, M. *Prog. Polym. Sci.* **2007**, *32*, 30. (e) Anselment, T. M. J.; Vagin, S. I.; Rieger, B. *Dalton Trans.* **2008**,

4537. (f) Gibson, V. C.; O'Reilly, R. K.; Reed, W.; Wass, D. F.; White, A. J. P.; Williams, D. J. *Chem. Commun.* **2002**, 1850. (g) Gibson, V. C.; Tomov, A.; Wass, D. F.; White, A. J. P.; Williams, D. J. *J. Chem. Soc., Dalton Trans.* **2002**, 2261. (h) O'Reilly, R. K.; Shaver, M. P.; Gibson, V. C.; White, A. J. P. *Macromolecules* **2007**, *40*, 7441. (i) Camacho, D. H.; Guan, Z. *Chem. Commun.* **2010**, *46*, 7879. (j) Guan, Z.; Popeney, C. S. *Top. Organomet. Chem.* **2009**, *26*, 179. (k) Lees, A. J. *Mol. Supramol. Photochem.* **2001**, *7*, 209. (l) Vlcek, A. Jr. *Coord. Chem. Rev.* **2002**, *230*, 225. (m) Hartl, F.; Rosa, P.; Ricard, L.; Le Floch, P.; Zalis, S. *Coord. Chem. Rev.* **2007**, *251*, 557. (n) van Slageren, J.; Klein, A.; Zalis, S. *Coord. Chem. Rev.* **2002**, *230*, 193. (o) Fedushkin, I. L.; Maslova, O. V.; Lukoyanov, A. N.; Fukin, G. K. *R. Chim.* **2010**, *13*, 584. (p) Trifonov, A. A. *Eur. J. Inorg. Chem.* **2007**, 3151. (q) Ward, M. D. *Coord. Chem. Rev.* **2010**, *254*, 2634. (r) Imbert, D.; Cantuel, M.; Buenzli, J.-C. G.; Bernardinelli, G.; Piguet, C. *J. Am. Chem. Soc.* **2003**, *125*, 15698.
- (2) van Koten, G.; Vrieze, K. *Adv. Organomet. Chem.* **1982**, *21*, 151.
- (3) Ittel, S. D.; Johnson, L. K.; Brookhart, M. *Chem. Rev.* **2000**, *100*, 1169.
- (4) Page, G.; Felix, A. M.; Dickie, D. A.; Chen, L.; Kemp, R. A. *Main Group Chem.* **2010**, *9*, 11.
- (5) Klerks, J. M.; Stufkens, D. J.; Van Koten, G.; Vrieze, K. *J. Organomet. Chem.* **1979**, *181*, 271.
- (6) Hill, N. J.; Vargas-Baca, I.; Cowley, A. H. *Dalton Trans.* **2009**, 240.
- (7) Shriver, D. F.; Drezdson, M. A. *The Manipulation of Air-Sensitive Compounds*, 2nd ed.; Wiley-Interscience: New York, 1986; p 336.
- (8) tom Dieck, H.; Renk, I. W. *Chem. Ber.* **1971**, *104*, 92.
- (9) tom Dieck, H.; Svoboda, M.; Greiser, T. *Z. Naturforsch., B: Chem. Sci.* **1981**, *36B*, 823.
- (10) Kliegman, J. M.; Barnes, R. K. *Tetrahedron* **1970**, *26*, 2555.
- (11) Beachley, O. T. Jr.; Rosenblum, D. B.; MacRae, D. J. *Organometallics* **2001**, *20*, 945.
- (12) APEX2; Bruker AXS, Inc.: Madison, WI, 2007.
- (13) Sheldrick, G. M. *Acta Crystallogr.* **2008**, *A64*, 112.
- (14) Spek, A. L. *J. Appl. Crystallogr.* **2003**, *36*, 7.
- (15) Brandenburg, K. *Diamond*, 3.1g; Crystal Impact GbR: Bonn, Germany, 1999.
- (16) Kanters, J. A.; van Mier, G. P. M.; Nijs, R. L. L. M.; van der Steen, F.; van Koten, G. *Acta Crystallogr.* **1988**, *C44*, 1391.
- (17) Hinchliffe, A.; Mair, F. S.; McInnes, E. J. L.; Pritchard, R. G.; Warren, J. E. *Dalton Trans.* **2008**, 222.
- (18) Gibson, V. C.; Redshaw, C.; White, A. J. P.; Williams, D. J. *J. Organomet. Chem.* **1998**, *550*, 453.
- (19) After we had deposited this structure into the CSD (661032), the structure was re-done and published, see: Olson, J. A.; Boyd, R.; Quail, J. W.; Foley, S. R. *Organometallics* **2010**, *27*, 5333.
- (20) (a) Baker, R. J.; Farley, R. D.; Jones, C.; Kloth, M.; Murphy, D. M. *J. Chem. Soc., Dalton Trans.* **2002**, 3844. (b) Bonello, O.; Jones, C.; Stasch, A.; Woodul, W. D. *Organometallics* **2010**, *29*, 4914.
- (21) (a) Clyburne, J. A. C.; Culp, R. D.; Kamepalli, S.; Cowley, A. H.; Decken, A. *Inorg. Chem.* **1996**, *35*, 6651. (b) Jenkins, H. A.; Dumaresque, C. L.; Vidovic, D.; Clyburne, J. A. C. *Can. J. Chem.* **2002**, *80*, 1398.